Evaluation of Optimum Packing Density for Cross-flow Hollow Fibre Membranes of Different Lengths Using CFD

Keng Boon Lim
Professional Officer, Professional Officers Division
Singapore Institute of Technology,
Singapore
KengBoon.Lim@singaporetech.edu.sg

Hui An
Lecturer, Engineering
Singapore Institute of Technology,
Singapore
Hui.An@singaporetech.edu.sg

Peng Cheng Wang*
Assistant Professor, Engineering
Singapore Institute of Technology,
Singapore
Victor.Wang@singaporetech.edu.sg

***Abstract*— In this study, the combined effect of packing density and fibre length were studied using CFD simulation. Hollow fibres with different combination of length and packing density were simulated to analyse the feed pressure and local flux distribution, as well as to predict permeate output flowrate. Simulation results showed that decrease in feed pressure along the membrane fibre was affected by both the fibre length and packing density. It was further revealed that fibres packed at 0.5 packing density had the highest permeate flow rate and the optimum packing densities of longer fibres were lesser than those of shorter fibres.**

Keywords-component; hollow fibre membrane; packing density; fibre length; CFD simulation

I. INTRODUCTION

Hollow fibre membranes are widely used in the filtration processes of waste water treatment [1]. Such membranes are designed to have very low aspect ratios (diameter to length ratio), in order to maximise the amount of fibres to fit into a module. This is desirable as a higher packing density indicates higher membrane surface area per unit volume, which ideally would lead to increased water flux and permeate flowrate, i.e. the two key parameters for optimisation of hollow fibre membrane modules (HHMM) [2,3]. However, research has shown that over packing of fibres leads to sub-par performance in terms of flux reduction and permeate velocity profile not fully developed [4,5]. In addition, hollow fibres come in different lengths for different domestic and industrial applications. This variation of length can also affect the output of hollow fibres.

Several authors have looked into how different packing densities affect the performance of hollow fibres membranes. Günther et al. [4] studied the changes in velocity profile at the permeate region of single fibres with different packing densities, a measure of expressing volume filled up by fibres as a fraction of total given volume Using computational fluid dynamics (CFD) simulations, they predicted that: (i) increasing packing density leads to non-uniform permeate profile along the fibre length, (ii) at packing densities of more than 0.6 (i.e. 60% of volume occupied by hollow fibre), filtration flux drops drastically and (iii) flux is higher at the fixed end of the hollow fibre.

Zhuang et al. [5] analysed the flux distribution in a dead-end outside-in HFMM through analytical model and CFD simulation. It was described that one of three different flux profiles could occur within the fibre, depending on the packing density: (i) uniform flux along length of hollow fibre, (ii) flux at dead-end is higher than flux at near the outlet and (iii) flux near the outlet is higher than flux at dead-end. Two dimensional axisymmetric models of hollow fibres with packing densities of 0.2, 0.4, 0.6 and 0.8 were simulated to study their flux profiles. They found that with the highest packing density of 0.2, the flux distribution fit the description in (i). Flux distribution of 0.4 packing density fit the description in (ii) while 0.6 and 0.8 packing densities fit the description in (iii). They also concluded that fibre diameter, length and packing density caused the non-uniformity of transmembrane pressure (TMP), which was directly proportional to the flux distribution.

Other than packing density, length of hollow fibre also affects the pressure distribution. Several past research have studied about how the length of fibre affects the pressure and flux distribution. Using analytical method, Carroll and Booker [6] derived a series of equations based on the Hagen-Poisseuille equation, that describes the permeate pressure, TMP and flux distribution. From their analysis, they concluded that for fibres that exceed 0.2 metres in length, pressure distribution was affected by the length of the fibre. This in turn leads to decrease in permeate flowrate per unit surface area as length increases.

Although research has been done to study the effects of varying packing densities and lengths, studies on the combined effects of both parameters were not done

*Corresponding Author

extensively. Studies pertaining to packing density were mostly done on short fibres (0.1 – 0.2 metres), in which length barely affects the performance of the fibre. Studies pertaining to fibre length were mostly done using standalone fibres. This ensures that fibre is adequately spaced so that results will not be affected by packing density. As industrial HFMMs are manufactured with long fibres (up to 2 metres) that are closely packed, it is apt to find out the most suitable packing densities for HFMMs of different fibre lengths.

For this study, the combined effects of different fibre lengths and packing density of outside-in hollow fibres will be studied. CFD models of hollow fibre with different combinations of length and packing density will be simulated. The authors aim to find the optimum packing density that can provide the highest permeate flowrate for the different fibre lengths studied.

II. METHODOLOGY

A. Numerical Approach

In this study, CFD simulations were conducted based on a model developed by Zhuang et al. [5]. The CFD model of the hollow fibre membrane was mainly developed with reference to Happel's free surface model [7], in which, each fibre within a bundle was modeled as a circular cell, consisting of a concentric fibre and its fluid envelope, as shown in Figure 1. In addition, fibres in the bundle were assumed to be uniformly spaced out, enabling the possibility to simulate only one fibre.

The CFD model created based on Happel's model was a 2D axisymmetric simplification of one fibre within the bundle. It consists of the feed and permeate region separated by the membrane (porous media) in between. All other boundary conditions are as shown in Figure 2. The change in packing density was achieved by changing the radius of the fluid envelope, r_o as denoted in Figure 1. The relationship between the packing density, φ and r_o was defined by the following equation [4 5]:

$$\Phi = \frac{\pi r_e^2}{2\sqrt{3}(r_o^2)} \qquad (1)$$

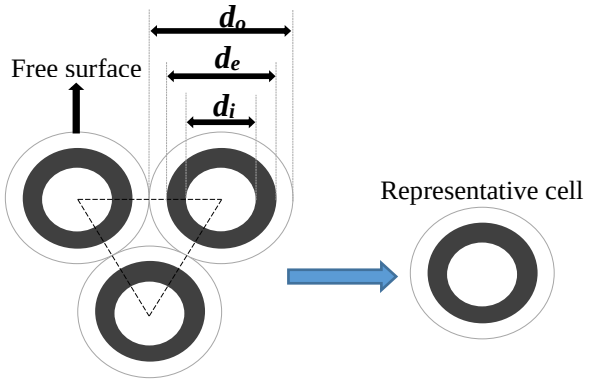

Fig. 1 Cross section of hollow fibre bundle as modelled by Zhuang et al. [5]. As fibres were assumed to be identical and uniformly packed, CFD simulation to be done on one representative hollow fibre.

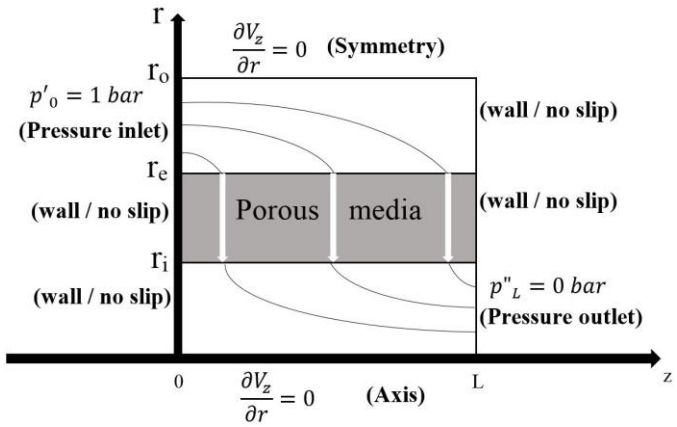

Fig. 2 Schematic layout of CFD model modelled by the same author [5].

Based on the model presented above, hollow fibres of four different lengths (0.5, 1, 1.5 and 2 metres) were modelled in the CFD domain. CFD models of each length was further modified to reflect the range of packing densities used in our study. The packing density ranged from 0.2 to 0.8, with an increment of 0.1 for each subsequent model. The resulting value for r_o was calculated using Equation 1. In total, 28 CFD models were generated, reflecting the combinations of different length and packing density used in this study. All other dimensions such as r_e and r_i were kept constant throughout at 7.5 x 10^{-4} metres and 3.125 x 10^{-4} metres respectively.

Mesh of CFD model was done in ANSYS 16.2. 21 and 16 nodes were distributed evenly along the radial direction of the membrane and permeate region respectively. As opposed to the 101 nodes distribution imposed in the original model from the literature, 1000 nodes were distributed along the longitudinal direction of the fibre for every 0.1 metres interval. This ensures better mesh aspect ratio and skewness, as the original nodal distribution produced elements with high aspect ratio and skewness which impeded convergence [8]. Node distribution along the radial direction for the feed region was dependent on the packing density, e.g. models with packing density of 0.2 had 31 nodes distributed evenly while models with 0.5 packing density had 11 nodes distributed evenly. This ensures that grid size is uniform regardless of fluid envelope radius, r_o.

Grid independence test was done using the CFD model generated for the hollow fibre with the length of 0.5 metres and packing density of 0.2. Refinement was mainly done at the interfaces between different regions. The size of the refined elements were chosen to be a quarter of the original element size. Comparison of results from simulations ran using both mesh showed percentage differences of 0.85% and 0.86% for the permeate flowrate at outlet and averaged flux of membrane respectively. A section of the medium mesh adopted is shown in Figure 3.

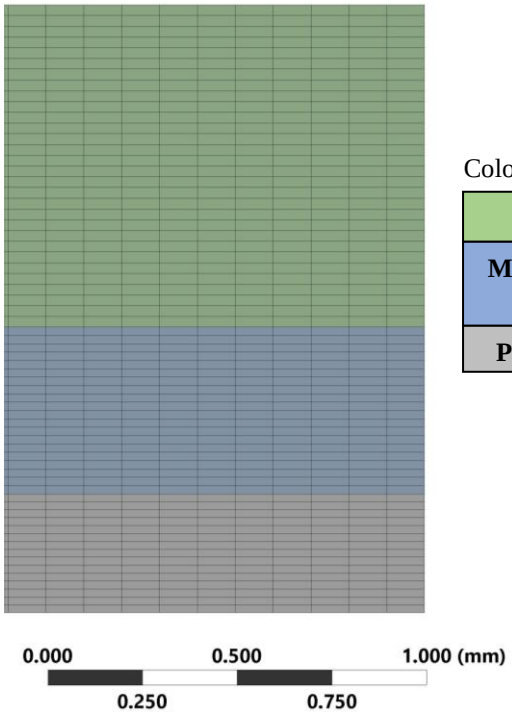

Fig. 3 Layout of medium mesh used in CFD simulation.

B. Boundary Conditions and solver settings used in CFD simulations

CFD models set-up were solved using the commercial CFD code FLUENT from ANSYS version 16.2. The inlet and outlet of the model was defined as 1 bar gauge pressure inlet (feed pressure) and 0 bar gauge pressure outlet respectively. All non-permeable surfaces, where water does not flow through, were set as wall with no slip condition. Cell zones of the CFD domain was defined to reflect the feed, membrane wall and permeate regions. The feed and permeate region were free moving spaces for fluid to move freely while the membrane wall region was defined as a porous media with permeability set at 1.802 x 10^{-15} m^2 and porosity at 0.7. Fluid used in simulation was pure water at 303.15K. This gives the density and viscosity to be 995.6 kg/m3 and 7.972x10-4 Pa.s respectively.

As past studies found in literature use the laminar model [4,5], the same model was used for the simulation. Pressure-velocity coupling with SIMPLE scheme was used for determination of pressure and velocity field. The "PRESTO!" scheme was selected as the interpolation method for pressure due to its suitability for flows involving steep pressure gradient. The second order upwind scheme was used for calculating velocity.

C. Theoretical Calculations

A theoretical model presented by Carrol and Booker [6] described the relationship between axial features such as fibre length and internal diameter, and the flux profile of hollow fibre membrane with the assumption of pure water flow. In [6], a series of equations were derived based on the model presented. As this theoretical model is very similar to the CFD model used, these equations were taken as reference to ensure consistency and validity of the author's results with literature. The following equations show the TMP and flux profile as a function of the length of a fibre:

TMP equation:

$$TMP(x) = P_f - P_p(x) = P_f \left[1 - \left(1 - \frac{\cosh\left\{ \sqrt{\frac{128\eta}{\pi}} \left(\frac{kLx}{d^2} \right) \right\}}{\cosh\left\{ \sqrt{\frac{128\eta}{\pi}} \left(\frac{kL}{d^2} \right) \right\}} \right) \right] \quad (2)$$

Flux equation:

$$\frac{dQ_f(x)}{dx} = k^2 L \left[P_f - P_p(x) \right] \quad (3)$$

III. VALIDATION OF RESULTS

Validation was done by comparing CFD results obtained against theoretical solutions calculated using Equations 2 and 3. Comparisons were made on TMP and flux distribution for the case of 0.5 metres fibre with 0.2 packing density. Fibres with packing density of 0.2 has less than 0.5% pressure drop along fibre length, and as such follows closely to the model from their literature, which assumes feed pressure to be constant throughout the fibre length [6].Theoretical values for TMP and local flux were calculated at every 0.0025 metres of fibre length. Figure 4 shows the close comparisons of theoretical calculation results against CFD simulation results. This gives confidence that the CFD methodology adopted here can be used for the analysis that will be discussed below.

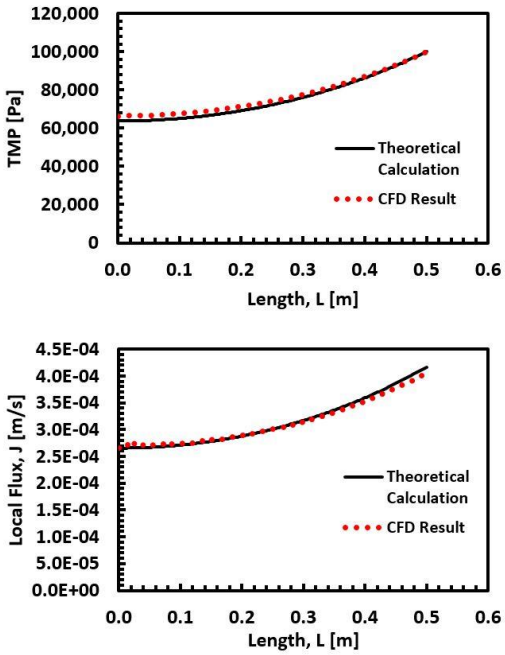

Fig. 4 Comparison of theoretical calculation results against CFD simulation results for (A) TMP and (B) local flux distribution of 0.5m fibre with 0.2 packing density.

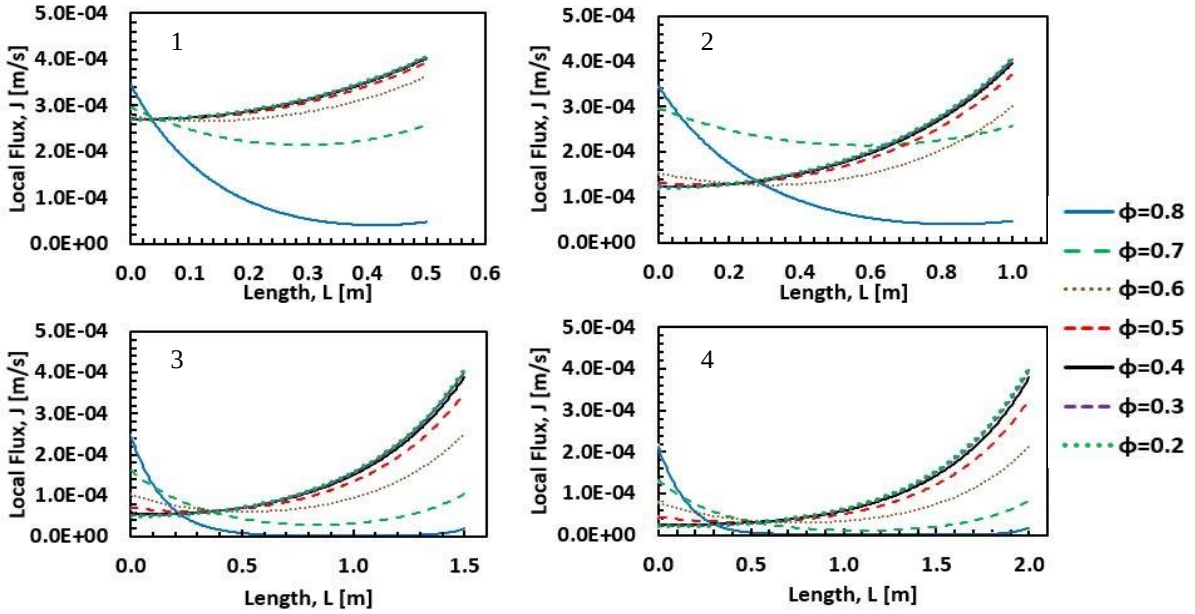

Fig. 5 Local flux distribution along length of fibre for (1) 0.5m, (2) 1m, (3) 1.5m and (4) 2m fibre respectively.

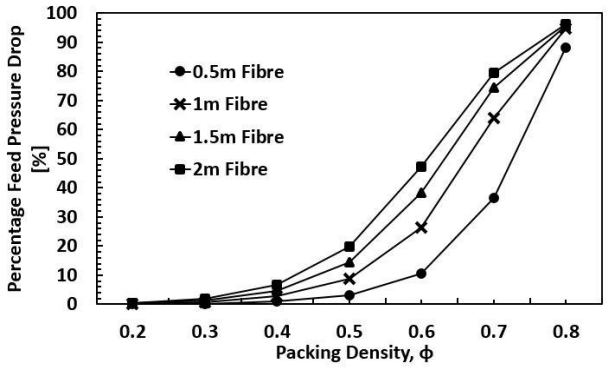

Fig. 6 Percentage feed pressure drop vs packing density for fibre lengths of 0.5, 1, 1.5 and 2 metres respectively.

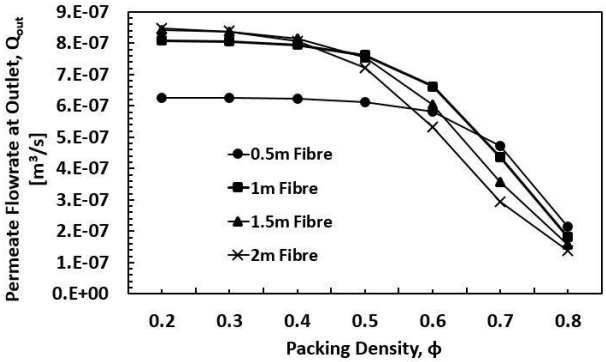

Fig. 7 Permeate flowrate at outlet vs packing density for fibre lengths of 0.5, 1, 1.5 and 2 metres respectively.

IV. RESULTS

A. *The effects of packing density on local flux distribution*

Using the CFD model presented in Section 2.2, results were obtained for models with different combinations of length and packing density.

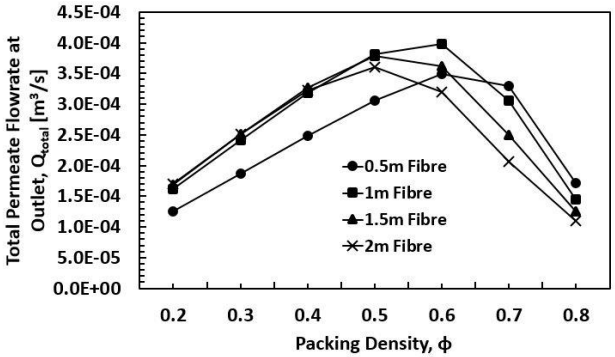

Fig. 8 Total permeate flowrate vs packing density for fibre lengths of 0.5, 1, 1.5 and 2 metres respectively.

Results show that significant change in the flux distribution can be observed when the packing density increases beyond 0.5, as seen in Figure 5. This is due to the large pressure loss in the feed region along the length of fibre as water travels through the narrow space, caused by over packing of fibres. This is further supported by Figure 4, which shows that the pressure drop along the fibre length in the feed region increases significantly as the packing density increases beyond 0.5. This led to a smaller margin of pressure difference available between both sides of the membrane, resulting in lower flux distribution [4].

B. *The effect of packing density on permeate flow rate*

Similar to local flux distribution, significant decrease in permeate flowrate can be observed when packing density goes beyond 0.5. As seen in Figure 7, for all fibre lengths studied, permeate flowrate remained stagnant up till packing density of 0.5, where the flowrate started to decrease significantly. As local flux distribution has a direct impact on permeate flow rate, the large reduction in feed pressure along fibre length has also leads to the drop in permeate flow rate.

C. *The effects of fibre length on feed pressure distribution*

Figure 6 also shows that the feed pressure drop mentioned in the sub section A increases proportionally with fibre length, for packing density of up to 0.7, as indicated by the proportional increase in the gradient. This indicates that fibre length is also a contributing factor to the reduction in feed pressure.

D. *Reverse flow pressent in membrane walls of long fibres caused by over packing*

As mentioned previously, longer fibres have larger drop in feed pressure along the length. The outcome is more adverse when the flux distribution of fibres packed at 0.7 and 0.8 packing density are studied. It is noticed in Figure 5, that segments with reverse flow are present for fibres of 1.5 and 2 metres long, when packed at 0.8 packing density. This indicates that a portion of water filtered is flowing back into the feed region. Such occurrence leads larger reduction in permeate flow rate of longer fibres as packing density increases. This is indicated in Figure 7, where 1.5 and 2 metres long fibres have a sharper drop in permeate flow rate at packing densities of 0.7 and 0.8, compared to fibres of 0.5 and 1 metre long.

E. *Packing density for Optimum Permeate Flowrate*

To evaluate the optimum packing density that gives the best permeate output, the relative permeate flowrate for each configuration of packing density and length was calculated. It is assumed that the total cross sectional area of a membrane module corresponds to the area of a bundle which could fit 1000 fibres with a packing density of 1.0. As mentioned before, since all fibres were assumed to be identical within each bundle, packing density will increase proportionally with number of fibres [2]. For example, a packing density of 0.8 corresponds to 800 fibres while packing density of 0.2 corresponds to 200 fibres. Using these assumptions, the relative total permeate flowrate was calculated as follows:

$$Q_{total} = Q_{out} \times N_{\phi=1} \times \phi \quad (4)$$

As shown in Figure 8, the best permeate outputs for the 0.5 and 1 metre fibres can be achieved at the packing density of 0.6, while for the 1.5 and 2 metres fibres, packing density of 0.5 seems to be the optimum. This is because fibres with a shorter length tends to have less flux reduction caused by the increase in packing density, as such, the permeate output from additional fibres is able to overcome this flux reduction. In addition, as shown in Figure 5 and Figure 7, at the packing densities of 0.5 and below, there are no significant changes in the local flux distribution and permeate flowrate, indicating that packing densities of less than 0.5 may cause under-utilisation of space available. On the other hand, packing densities of more than 0.6 may result in over packing of the fibres, leading toe large reduction in the feed pressure along the fibres which in turn limits the transmembrane pressure: the force driving the water through the membranes.

V. CONCLUSION

Hollow fibres of different length and packing densities were studied using numerical methods, with the aim of estimating the optimum packing density for each fibre length studied.
From result obtained through CFD simulation, the follow conclusions were made:

i) Reducing packing density below 0.5 does not provide significant changes to feed pressure, local flux distribution and permeate flowrate.
ii) Increasing packing density above 0.6 may cause drastic drop in feed pressure along the fibre length. This pressure drop is also affected by fibre length. At the same packing density, longer fibre have larger feed pressure drop than shorter fibres.
iii) The drop in feed pressure limits the transmembrane pressure across the two sides of the membrane, reducing permeate flowrate of said fibre.
iv) Reverse flow along the membrane wall will occur on fibres longer than 1.5 metres at extremely dense packing density ($\phi > 0.8$)
v) Fibre bundles with packing densities of 0.5 and 0.6 provided the most permeate output for all fibre length studied. Fibres packed at this density range maximised the space available, while making minimum sacrifices to performance reduction for individual fibres.

ACKNOWLEDGMENT

The authors acknowledge the Enterprise and Innovation Hub (E.I. Hub), Singapore Institute of Technology for their support and funding (E.I. Hub Ignition Grant) for this research project.

NOMENCLATURE

K	Membrane permeability (m^2)
L	Length of fibre (m)
$N_{\Phi=1}$	Number of fibres for packing density of 1
P_f	Pressure at feed region (Pa)
P_p	Pressure at permeate region (Pa)
Q_f	Flowrate of feed through membrane wall
Q_{out}	Permeate flowrate at outlet
Q_{total}	Relative total permeate flowrate at outlet
r_i	Internal radius of fibre (m)
r_e	External radius of fibre (m)
r_o	Outer boundary radius of fluid envelope (m)
x	Dimensionless axial position coordinate [4]
φ	Packing density
η	Dynamic viscosity of water (Pa.s)

REFERENCES

[1] Anthony M. Wachinski, 2013, Membrane Processes for Water Reuse. Published by Mc Graw Hill Companies, In

[2] M. R. Doshi, W. N. Gill and V. N. Kabadi, Optimal Design of Hollow Fiber Modules. AlChE J. 23 (1997) 765- 767

[3] M. Soltanieh, W. N. Gill, A note on the effect of fibre length on the productivity of hollow fibre modules, Chem. Eng. Commun. 22 (1983) 109

[4] Jan Gunther, Philippe Schmitz, Claire Albasi and Christine Lafforgue, A numerical approach to study the impact of packing density on fluid flow distribution in hollow fibre module, J. Membr. Sci. 348 (2010) 277-286.

[5] Liwen Zhuang, Hanfei Guo, Penghui Wang and Gance Dai, Study on the flux distribution in a dead-end outside-in hollow fibre membrane module, J. Membr. Sci. 495 (2015) 372-383.

[6] T. Carroll and N.A. Booker, Axial features in the fouling of hollow fibre membranes, J. Membr. Sci. 168 (2000) 203-212.

[7] J. Happel, Viscous flow relative to arrays of cylinders, AlChE J. 5 (1959) 174-177.

[8] ANSYS Inc, ANSYS 16.2 Help, 20.2.4. Quality Measure (2016).